Extrusion of aluminium hollow pipes: seam weld quality assessment via numerical simulation

Silvia Bozzi *, Maurizio Vedani **, Daniele Lotti *, Giuseppe Passoni ***
***Hydraulic Lab. - DIIAR, Politecnico di Milano, Milano, Italy**
****Department of Mechanical Engineering, Politecnico di Milano, Milano, Italy**
*****Dynamic Technologies Group, Udine, Italy**

ABSTRACT

The continuous extrusion of an aluminium alloy for hollow tubes production was investigated by numerical simulations. A variety of model runs were carried out exploring different combinations of die geometries and extrusion speeds. The primary objective of this work was to compare different criteria for evaluating the quality of longitudinal seam welds. The results of the numerical experiments show that the currently used quality indices, based on the integration of some characteristic variables across the welding surface are significantly affected by the extension of the dead flow zones. As a result, they do not behave coherently with respect to changes in shapes of the mandrel legs. The use of a novel Lagrangian approach in the estimation of the quality indices - based on the integration of the variables along the actual welding paths - leads to a more consistent behavior of the parameters with respect to both the extrusion velocity and the front leg shape. In this study we also show that the Lagrangian parameters can be applied to get a deeper insight into the quality of the extruded products, like the seam weld quality along the tube thickness. Further research is needed to investigate the relation between the Lagrangian quality indices and the microstructure of the material.

RIASSUNTO

Viene analizzata, con l'ausilio della simulazione numerica, la produzione di tubi a sezione cava in lega di Alluminio mediante il processo di estrusione continua. Sono state simulate varie combinazioni di geometria della matrice e di velocità di estrusione. Il principale obiettivo del presente lavoro è quello di confrontare vari criteri per la valutazione della qualità della saldatura longitudinale. I risultati delle simulazioni numeriche mostrano che i criteri di qualità attualmente utilizzati, basati sull'integrazione di alcune variabili caratteristiche perpendicolarmente alla superficie di saldatura, sono influenzati in modo significativo dalla presenza delle aree in cui il flusso plastico di materiale presenta velocità molto basse. Di conseguenza questi parametri rispondono in modo incoerente alle variazioni di forma del supporto del maschio centrale. L'utilizzo di un approccio Arrangiano per la valutazione degli indici di qualità – basato sull'integrazione delle variabili in direzione dell'effettiva linea di saldatura – porta ad un comportamento più coerente dei parametri sia riguardo alla velocità di estrusione, che alla geometria della matrice. Nel presente studio si dimostra anche che i parametri lagrangiani possono essere utilizzati per uno studio approfondito della qualità dei prodotti estrusi, come la valutazione del cordone di saldatura lungo lo spessore del tubo. Ulteriori attività di ricerca sono necessarie per individuare la relazione tra gli indici di qualità lagrangiani e la microstruttura del materiale.

KEYWORDS

Aluminum alloy; Extrusion; Welding criteria; Numerical simulation; Microstructure.

INTRODUCTION

Aluminium extrusion is one of the most widely used processes for manufacturing complex solid and hollow shapes. The process converts a cast billet of a metallic alloy into a profile of uniform cross-section by forcing it to flow through a die orifice under high pressure and high temperature. A special case in the extrusion of aluminum alloys is the production of hollow sections. Tubes are extruded by means of hollow dies having a stationary core or mandrel, which determines the inner circumference of the profile. The mandrel is firmly kept in its position by legs or bridges, embedded in the back of the die. When the aluminium billet is pushed in the die, the material flow splits into different streams around the mandrel supports. Past the mandrel, the

metal streams rejoin in the welding chamber and become welded in the solid state by the effect of pressure and temperature. As a result, unavoidable extrusion welds are generated in the profiles, corresponding to the location of each leg (Fig. 1). Extrusion welds are considered to be one of the most critical regions of extrudates. Defects and structural inhomogeneities at seam welds become apparent after anodizing in the form of streaking along the extrudate [1] and reduce part ductility and fatigue strength [2, 3]. The weld quality depends on a complex combination of thermal and mechanical parameters inside the die and especially in the welding chamber. In order to assure proper welds, a variety of factors should be considered related to die design, such as weld chamber shape and bridge geometry and to process parameters such as temperature and extrusion speed [4]. The same parameters also influence the cost and productivity of the process and so the optimum is given by a proper balance between the section quality and the cost efficiency of the extrusion plant.

During the last decades, a better understanding of the extrusion process has come from mathematical modelling. Numerical simulations allowed to predict the spatial distribution of pressure, velocity and temperature in a given geometry, which are the primitive variables for deriving the stress-strain histories of the deformed metal. In numerical simulations, two approaches can be used: the solid or Lagrangian formulation, which describes the movement and deformation of a rigid body and the fluid or Eulerian formulation, which treats the metal as a non-Newtonian fluid. A detailed analysis of both solid and fluid formulations and their applications to different forming processes in two and three dimensions can be found in Kobayashi [5]. The Lagrangian numerical calculations are performed when both elastic and plastic deformations are of interest such as in the modeling of the bearing area [6] or when the total strain history is important, such as in simulations of microstructure evolution [7, 8]. In the other cases, the numerical analysis of the process can be carried out more easily and efficiently with an Eulerian approach [9]. In fact, given that the stresses generated through plastic deformation at high temperatures are almost independent of total strains and that elastic strains are small compared to the large plastic deformations occurring during the process [10], the metal can be properly described as a rigid-plastic or rigid-viscoplastic fluid. Since the earlier works of Goon [11] and Zienkiewicz and Godbole [12] the flow formulation has been widely used in the analysis of the aluminium extrusion process [9, 13, 14].

Thanks to the detailed three-dimensional simulations, with either solid or fluid formulations, carried out in recent years, a better knowledge of the phenomena occurring during extrusion was achieved. However, the relationships between the metal flow variables and the quality and properties of the extruded hollow profiles are still poorly understood. Once the results of the numerical experiments are obtained, the main problem is to relate the large amount of information that the simulations provide (flow patterns, velocity and pressure fields, deformation histories, etc.) to the quality of the final products. A new methodology for the prediction of weld quality in extruded Al-Mg-Si alloys was recently proposed by Donati and Tomesani [15] based on thermo-mechanical FEM analyses. Parameters such as pressure, flow stress and velocity in the welding chamber were taken into account in a criterion for weld quality. In a later paper [16], the same authors investigated experimentally the effect of different welding chamber geometries and process conditions on the mechanical properties of the extruded profiles.

From this background, the aim of this work is to investigate the reliability of different quality criteria by means of numerical simulations. We focused on the extrusion of tubes of aluminium alloys, for which the mechanical properties of the final product strongly depend on the quality of the longitudinal weld lines. We carried out four sets of simulations - combining two different geometries of mandrel supports and two process speeds - and for each case we calculated the seam welds quality criteria proposed in literature [15, 17]. By comparison of the model results, we elucidated which are the key process parameters affecting seam welds and which are the most appropriate criterion to assess the quality of extruded tubes. We also coped with the problem of homogeneity of the tube cross-section by computing the welding quality parameters along the tube thickness.

The paper is organized as follows: in section 2 the mathematical method used for the simulations is presented; in section 3 the experimental data are described; in section 4, we provided the details of the existing criteria of seam weld quality; in section 5 we presented the results of the metal flow simulations in terms of welding quality indices and some conclusions are drawn.

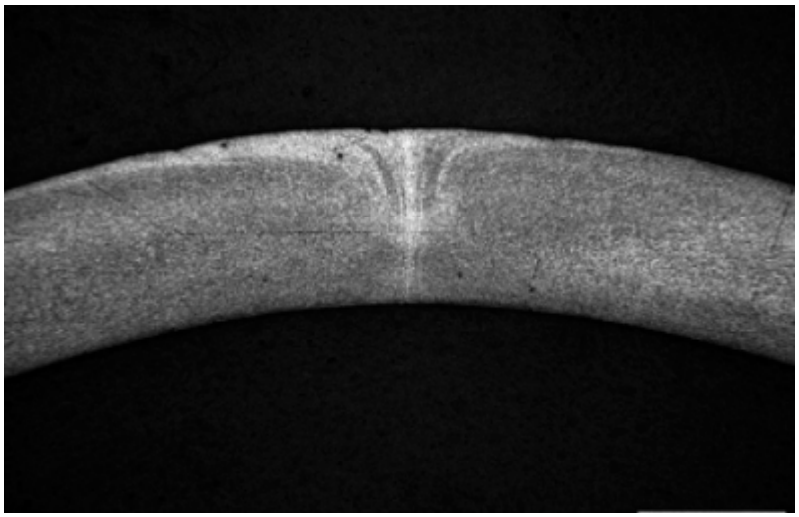

Fig. 1: Weld seam found on a cross-sectioned tube sample.

NUMERICAL SIMULATIONS

In the present work the continuous extrusion of aluminium circular hollow section - diameter of 20 mm and a thickness of 1 mm - was investigated.
Fig. 2 illustrates the essence of the process. The machine has a rotating wheel (1) with a circumferential groove enclosed by a fixed shoe (3). A continuous feedstock (2) is forced into the groove by means of a coning roll and it is driven down by the friction between the feedstock and the feeder plate (4). Then the movement of the fed material is blocked by an abutment (6), which forces the metal into the expansion chamber (5) and then through the die as a final product (7). A part of the feed material is also extruded through the clearance gap between the shoe and the wheel (7). The presence of four resistors in the shoe and the friction heat generated near the abutment ensure that the metal can be properly formed.
In these conditions, the aluminium can be treated as an incompressible non-Newtonian fluid and the motion can be adequately described by the constitutive equation of the material and by the conservation laws for mass, momentum and energy. For a steady state problem, the conservation equations can be written respectively as:

$$\nabla \cdot \mathbf{u} = 0$$
$$\rho(\mathbf{u} \cdot \nabla)\mathbf{u} = -\nabla p + \nabla \cdot \sigma \qquad (1)$$
$$\nabla \cdot (\rho u c_p T) = \nabla \cdot (k \nabla T) + \text{viscous term}$$

where **u** is the velocity vector, p is pressure, σ is the stress tensor, T is temperature, ρ is density, c_p is specific heat and k is thermal conductivity.
The most widely used constitutive laws for hot aluminium are viscoplastic approximations, which neglects the elastic behavior of the material. The description of viscoplastic flow assumes that the deviatoric stress tensor **s** and the rate of deformation tensor **e** can be related by the following linear equation:

$$\mathbf{s} = 2\mu\mathbf{e} \qquad (2)$$

where μ is a non-constant viscosity, dependent on temperature and strain rate.

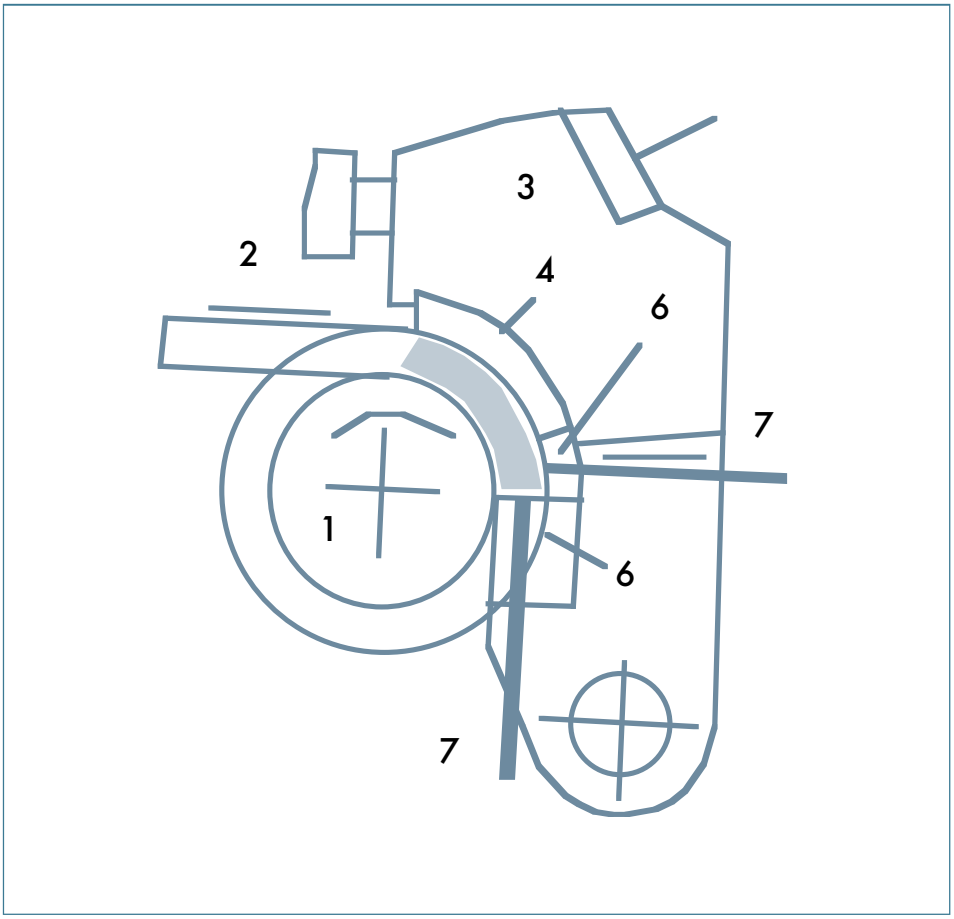

Fig. 2: Schematic representation of the continuous extrusion process. (1) rotating wheel, (2) feedstock, (3) shoe, (4) feeder plate, (5) expansion chamber, (6) abutment, (7) extruded product.

Introducing the equivalent stress $\bar{\sigma}$ and strain rate $\dot{\bar{\varepsilon}}$ defined respectively by:

$$\bar{\sigma} = \sqrt{3/2\, s:s} \qquad (3)$$
$$\dot{\bar{\varepsilon}} = \sqrt{2/3\, e:e}$$

the following constitutive equation can be derived:

$$\mu(\dot{\bar{\varepsilon}}, T) = \sigma / 3\dot{\bar{\varepsilon}} \qquad (4)$$

The deformation of aluminium alloys during hot extrusion is commonly described by the Sellars and Tegart law [18], later modified by Lof [6] to introduce an elastic yield stress:

$$\bar{\sigma} = \sigma_0 \operatorname{arcsinh}\left[\left(\frac{\dot{\bar{\varepsilon}} + \dot{\bar{\varepsilon}}_0}{A}\exp\left(\frac{Q}{RT}\right)\right)^{1/n}\right] \qquad (5)$$

In this equation Q is the activation energy for deformation, T is temperature, R is the universal gas constant (8.314 J mol^{-1} K^{-1}) and σ_0, n, and A are material constants. Finally, to close the governing equations we also calculated the temperature field inside the shoe, solving the heat conduction equation.
The material parameters used in the simulations refer to the AA3103 commercial alloy are reported in Table 1. The parameters of the constitutive equation (Q, ε_0, σ_0, n, and A) were set according to Sheppard [4].
The commercial CFD code FLUENT™ [19] which is based on the finite volume method, was used for solving the set of governing equations in a three dimensional domain. The program uses a segregated solver approach, that consists in solving the

conservation equations of mass and momentum separately one at a time in a decoupled iterative procedure until a converged solution is obtained. In our simulations the PISO algorithm [20] was used for the pressure-velocity coupling and second order accurate upwind differencing schemes were chosen as spatial interpolation methods. Convergence was evaluated by examining the residual levels of the state variables and by monitoring the evolution of different integrated quantities at the outlet section. To speed up the convergence we first computed the isothermal flow field, then we calculated the only energy field and finally we solve the whole system of coupled equations (1).
The flow boundary conditions were set as follows: at the inlet a constant velocity of the billet is prescribed, at the walls fully sticking is assumed, i.e. a no-slip condition is imposed and at the outlet a zero pressure gradient is specified. Given the symmetry of the geometry, only one half of the whole domain is simulated and a free-slip and zero normal velocity is imposed on the symmetry plane.
In the energy equation the following boundary conditions are imposed: constant aluminium temperature at the inlet, prescribed heat flux at the resistors, zero temperature gradient at the outflow, local thermal equilibrium at the internal walls forming the interface between the aluminium and the shoe and a convective heat transfer condition at the external wall boundaries. The latter condition corresponds to imposing a heat flux at the walls, given by the following expression:

$$q = h_{ext}(T_{ext}-T) \quad (6)$$

where T is the surface temperature of the wall, and T_{ext} and h_{ext} are given constants representing respectively the temperature and the heat transfer coefficient of the external free stream.
The described model was used to carry out four simulations, representing different combinations of die geometries and extrusion conditions. As shown in Fig. 3, the geometries differ for the angle of the front legs of the mandrel, which is lower in G2 (30°) with respect to G1 (90°).
Depending on the die design, a slightly different condition at the resistors was imposed. For each geometry we simulated the process at two different extrusion speed

Table I. Material parameters used in the simulations.

Aluminium	ρ [kg m^{-3}]	2730
EN AW	k [W m-1 K-1]	160
AA3103	c_p [J kg-1 K-1]	890
alloy	σ_0 [MPa]	31
	A [s^{-1}]	9.4 x 1012
	Q [J mol^{-1}]	183100
	n [-]	4.96
	ε_0 [s^{-1}]	0.005
Steel	ρ [kg m^{-3}]	7700
H-13	k [W m^{-1} K^{-1}]	29
	c_p [J kg^{-1} K^{-1}]	503

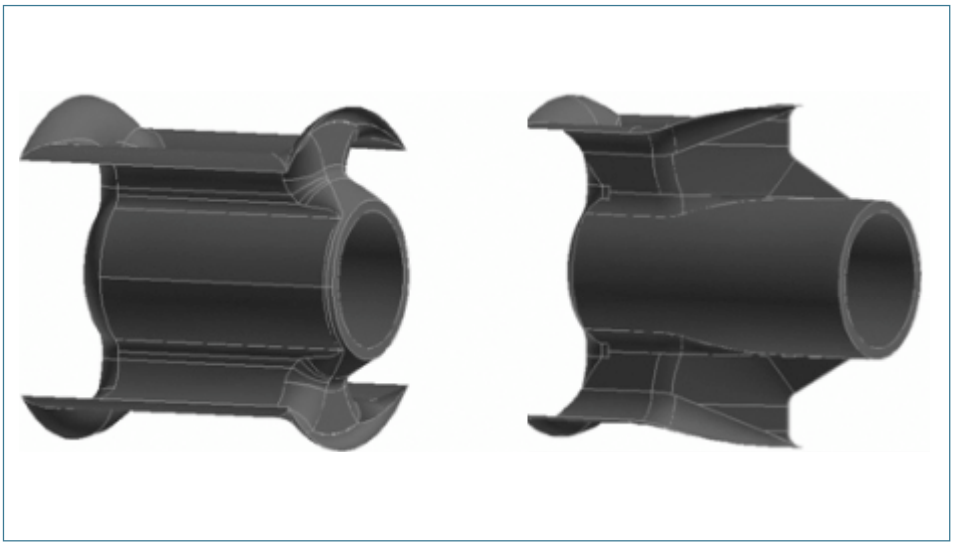

Fig. 3: 3D views of die geometries G1 (left) and G2 (right), flow direction from left to right.

V1 and V2, corresponding to 9 and 11 rpm of the rotating wheel, respectively. The input data and the boundary conditions for the four simulations are reported in Table 2. In the discussion below, individual runs will be referred to as GiVj, where G and V represent geometry and extrusion speed and i, j denote the individual data sets.

Table 2. Simulation parameters.

G1V1	**G1V2**	**G2V1**	**G2V2**	
Mandrel leg angle	90°	90°	30°	30°
Resistor power [W]	840	840	950	950
Wheel speed [rpm]	9	11	9	11
Billet velocity at the inlet [m/s]	0.14	0.17	0.14	0.17
Billet temperature at the inlet [°K]	298	298	298	298
Free stream heat transfer coefficient [W/m2 °K]	10	10	10	10
Free stream temperature [°K]	298	298	298	298

EXPERIMENTAL ANALYSIS

Samples of the tubes produced by extrusion of AA3103 alloy in an industrial plant with G1V1 conditions, were analyzed to investigate the main features of their microstructure. For this purpose, transversal and longitudinal sections were cut from the tubes by a diamond-blade saw and prepared for analyses.

The macrostructure of the weld seams (Fig. 1) was revealed by fine-grinding the cross section of the tubes and by etching the surface with a 25% NaOH-75% water solution at 60°C. For microstructural observations, the samples were polished to a 1 μm finish and then anodized in a 2%HBF4 water solution at a potential of 25V. An optical microscope operating with polarized light was used to take representative micrographs along the thickness of the samples.

Fig. 4 shows a typical view of a cross-sectioned sample obtained by optical microscopy, revealing that the extruded alloy microstructure featured a bimodal grain size distribution. A region close to external and internal surfaces of the tube always showed a layer of coarse grains while at the interior of the tube wall, much finer equiaxed grains with a size of about 15 μm could be recognized. The occurrence of a coarser structure at the surface of extrudates is a well known feature called peripheral coarse grain (PCG) structure that is usually accounted for by the process of grain growth during high-temperature processing of the alloy. Occasionally, within the central fine-grained region, isolated coarse grains were also noticed, suggesting that secondary recrystallization (also known as abnormal grain growth) took place during the last stages of tube processing [21].

Careful analysis of the microstructure of the samples at the position of the weld seam did not revealed any significant difference in grain size distribution with respect to the structure found in other regions of the tube. It is therefore supposed that the macroscopic contrast observed on macroscopic views revealing the weld position (see Fig. 1) could be due to a more pronounced etching effect stimulated by a larger amount of small intermetallic particles that were not revealed by polarized light observations [1].

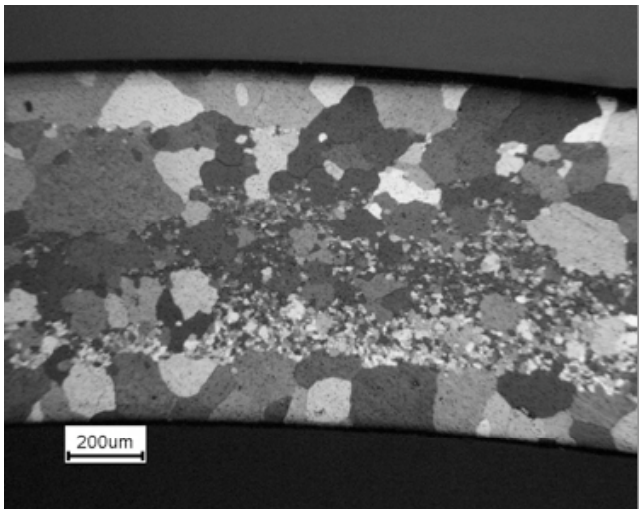

Fig. 4: Optical micrograph of the alloy structure along the sample thickness.

QUALITY CRITERIA FOR LONGITUDINAL EXTRUSION WELDING

During the extrusion of hollow sections, the aluminium flow divides into separate streams, which flow around the mandrel supports and then weld together before passing through the die. This method creates in the extruded profiles longitudinal welds corresponding to the location of each leg. The quality of the end product depends on the strength of the seam welds, which in turn depends on the stress-strain history along the axis of extrusion and on the geometry of the welding chamber and mandrel supports.

The first criterion for the quality of seam welds has been proposed by Akeret [22]. He suggested that proper welding occurs when the maximum pressure inside the welding chamber exceeds a threshold, which depends on the state of deformation of the aluminium at that point.

$$A = \max(P) \qquad (7)$$

Then Plata and Piwnik [17] proposed a more elaborate index, based on the whole deformation history of the material and on the contact time after equalization of the streams. In fact, as aluminium has viscoplastic behavior, the material stops flowing when the extrusion force is relaxed so that stresses fall below the yield point. The proposed criterion is calculated by time integrating the rating of contact pressure P to effective stress $\overline{\sigma}$, along a generic welding path:

$$PP = \int_t P/\overline{\sigma} \cdot dt \qquad (8)$$

The index must exceed a critical threshold in order to ensure proper welding.

Bourqui et al. [14] suggested that healthy weld seams are obtained when pressure in the weld chamber exceeds half the die entrance pressure. They also noticed that as the PP index does not take into account the length of the paths of the rejoining streams, the critical value of the parameter should depend on the length of welding chamber, being higher for longer chambers.

Recently, Donati and Tomesani [15] compared different methods for evaluating seam weld quality in aluminium extruded profiles and proposed the following criterion:

$$DT = \int_t P/\overline{\sigma} \cdot \nu \cdot dt = \int_s P/\overline{\sigma} \cdot dt \qquad (9)$$

where ν is the velocity along the welding path and s is the spatial coordinate along the path from the back side of the die leg to the die exit. The speed velocity was introduced to weight the ratio of pressure to effective stress according to the residence

time, thus reducing the importance of the low velocity areas. The authors performed the calculations of the *PP* and *DT* parameters by using the following discrete forms of equations (8) and (9):

$$PP = \sum_{i=1}^{l} \sum_{j=1}^{m} \frac{P_{ij}}{\bar{\sigma}_{ij} v_{ij}} \qquad (10)$$

$$DT = \sum_{i=1}^{l} \sum_{j=1}^{m} \frac{P_{ij}}{\bar{\sigma}_{ij}}$$

where *l* and m represent the elements of the welding surface. The authors carried out a series of FEM simulations reproducing the Valberg tests [23, 24] and they showed that the *DT* index, normalized by the welding chamber width, is the only parameter in fully accordance with the experimental evidences.

In the present work, we estimated the *PP* and *DT* parameters by using the results of the numerical simulations. According to Donati and Tomesani [15], the indices were evaluated by using the distribution of the characteristic variables (contact pressure, effective stress and velocity) on the welding plane between the reconnection of the metal flow. The same parameters were also calculated on a Lagrangian basis, obtaining respectively the *PP** and *DT** indices. For this purpose, N tracer particles (~10^3) were introduced from the cross section located at the end the mandrel supports, where the metal streams start to rejoin and they were tracked until the die exit (Fig. 5). Among these particle trajectories we selected the ones ending on the seam weld line (blue lines in Fig. 5), corresponding to the welding paths. The Lagrangian welding parameters were computed by calculating the characteristic variables along the trajectories from the points where they were closer than 0.1 mm (10% of tube thickness) to the contact surface to the die exit (red lines in Fig. 5). Then we integrated in time or space the variables, according to the equations (8) and (9), to obtain respectively the *PP** and *DT** indices of each welding path. Finally, the arithmetic mean of the N parameters of each particle trajectory was considered as the mean quality index of the extruded section.

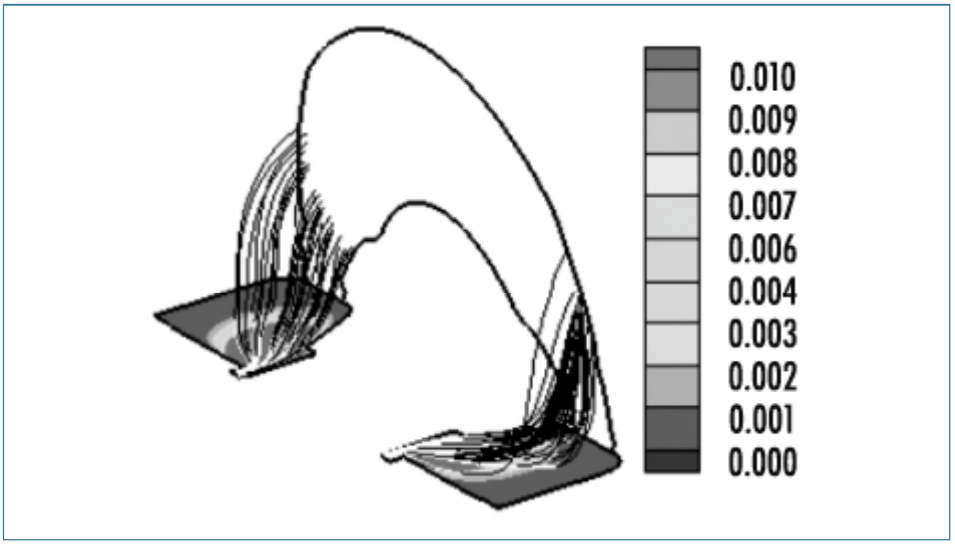

Fig. 5: Contours of velocity magnitude [m/s] on the welding surface and trajectories of the welding paths. White color refers to the portion used in the computation of the lagrangian welding indices.

RESULTS AND DISCUSSION

SEAM WELD QUALITY

The quality indices, as calculated from the numerical simulations, are reported in Fig. 6. A first comparison shows that they are more affected by changes in leg shapes than in process speeds. This agrees with previous works indicating that the mechanical properties of extruded hollow profiles are mostly influenced by die geometry (e.g. [16]).

All the parameters decrease as velocity increases from 9 rpm to 11 rpm, for both geometries, as expected. Particularly, *PP* decreases by more than 10%, *DT* by about 2% and the Lagrangian indices exhibit a reduction less than 1%.

On the other hand, not all the parameters behave similarly with respect to changes in bridge geometry. If the 30° leg angle is used instead of the square one, the Eulerian criteria predict a reduction of the seam weld quality, while the Lagrangian criteria exhibit an opposite trend. Therefore, the behavior of the Eulerian indices *PP* and *DT* contrast with the experimental results of previous works [22, 16], where an improvement of the welding quality by reduction of the leg angle is reported.

The reason for the different behavior of the Eulerian and Lagrangian indices with respect to the die geometry seems to be the different relative weight given to the dead flow zones in the index calculation. The dead metal zones are areas of very low velocities which are typically found along the outer walls of the welding chamber. As can be seen in Fig. 5 these zones are characterized by large velocity differences with respect to the neighboring zones. The *PP* criterion is significantly influenced by the dead metal zones because it is formulated as a time integral: the differences between the *PP* index calculated for the G1 and G2 geometry are extremely high, almost 100%. The *DT* criterion consists in a space integral and so it does not explicitly depend on the fluid residence time on the welding surface. As a consequence, although the *DT* index is still not consistent with the changes in leg shapes, the difference between the two geometries is reduced to 30%. The spatial distribution of *DT* on the welding surface, for the G1V1 and G2V1 simulations, shows that the most important differences are concentrated in the dead zones (Fig. 7). Hence, the *DT* criterion is deeply affected by the behavior of the flow in the dead zones, even if the metal residing in these areas do not flow into the weld seams (Fig. 5). In fact, the welding paths do not extend all over the welding surface but are concentrated in the inner half of the welding plane, which excludes the dead zones.

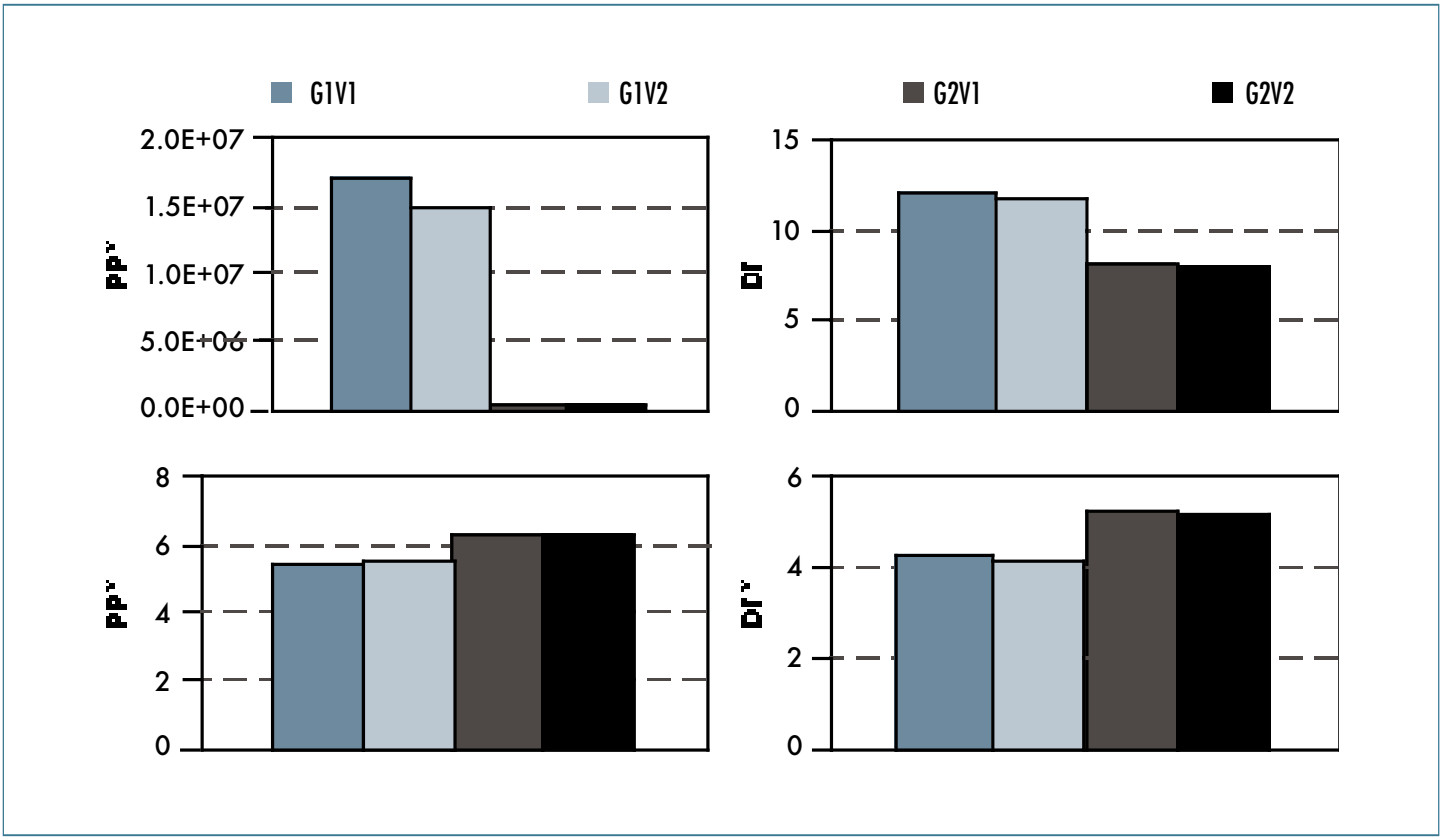

Fig. 6: Comparison between welding quality indices.

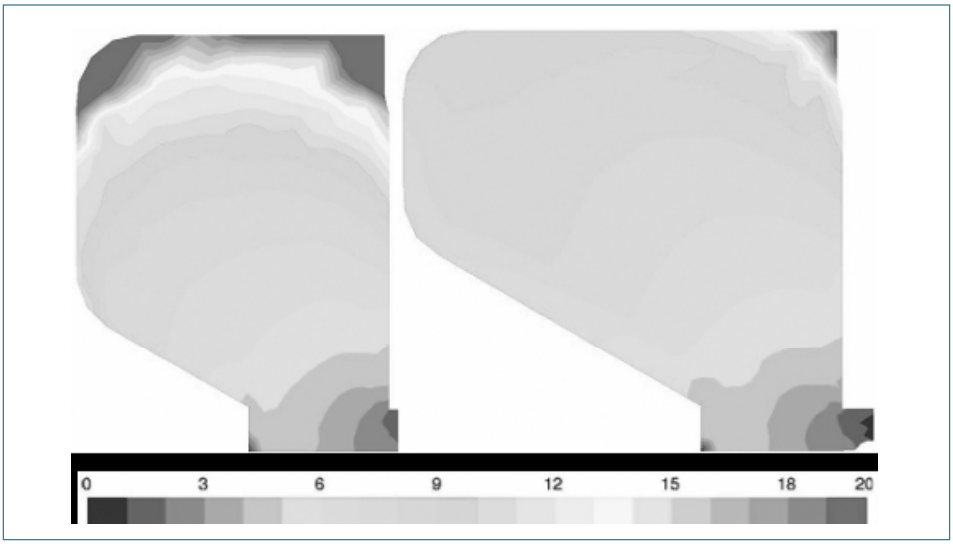

Fig. 7: *DT* index on the welding surface, for G1V1 and G2V1 simulations.

In conclusion, the integration of the quality parameters over the whole welding plane can give misleading results because it takes into account a wide portion of the surface, which actually does not contribute to form the weld seam line. On the other hand, the Lagrangian approach, based on the integration of the variables in space or time, along the welding paths assures that the indices are calculated including the actual portion of the welding surface occupied by the rejoining streams.

WELD QUALITY ALONG THE WALL THICKNESS

The Lagrangian approach used to estimate the *PP** and *DT** indices also permits to assess the weld quality along the tube thickness. In fact, the particle trajectories end at different positions along the seam line. At each final location corresponds a value of the quality index, resulting from the whole thermo-mechanical history of the particle. Fig. 8 shows the distribution of the *DT** parameter along the tube thickness for

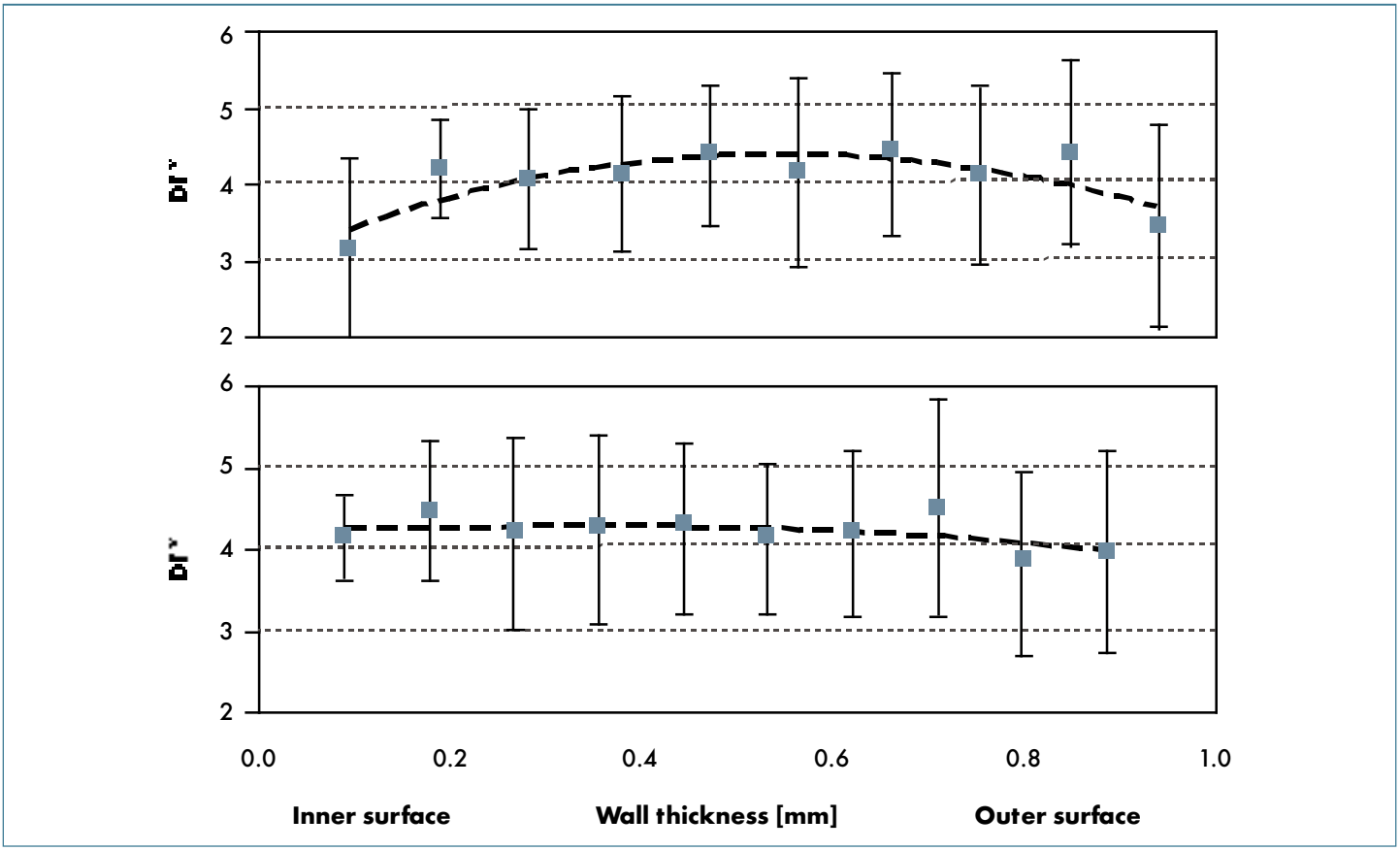

Fig. 8: *DT** index along the wall thickness, for the upper (a) and lower (b) weld seams. Solid squares represent class averages, vertical lines show standard deviations and dashed lines are polynomial trends.

the base simulation G1V1, obtained by subdividing the particles into 10 classes, equally spaced along the seam line. The behavior of the *PP** parameter is not presented here because it shows the same trend, for both the lower and upper seam welds. The figure shows that the *DT** distribution is not the same for the two lines: the quality index exhibits a convex trend in the upper line but it is almost constant along the lower line. The average value of the *DT** index is 5% higher for the lower seam weld. The reason of this behavior is due to the different histories of the fluid streams forming the two extrusion welds. In the continuous extrusion process the presence of the abutment determines different conditions of the flow entering at the top and at the bottom of the expansion chamber. The fluid in the higher part is subjected to lower pressure fields and higher strain rates (and so higher effective stresses) and these conditions can be found along the whole chamber length, up to the die exit and in the final product. Therefore, the upper seam weld is characterized by worst quality than the lower one, because the ratio between normal and effective stresses is lower during the welding paths, as a result of the history of the flowing material.

The distribution of the *DT** parameter along the top seam weld shows a better quality of the tube in the central region and a worse quality at the two peripheries. It is worth to observe that this behavior reasonably matches the typical grain size distribution of the material observed by optical micrographs, where coarse grains layers are close to the external and internal surfaces of the tube (Fig. 4). A similar trend can not be found in the lower seam line despite to the fact that the bimodal grain size distribution characterize the whole tube cross section. Additional studies are needed to ascertain the relation between the Lagrangian welding quality parameters and the microstructure of the material due to the recrystallization process.

CONCLUSIONS

A set of numerical simulations of the continuous extrusion process of an aluminium alloy has been carried out to investigate the performance of different criteria for seam weld quality prediction. The behavior of two recently proposed quality indices was analyzed with respect to changes in process speed and front leg shape. Both the parameters take into account the ratio between the normal pressure and the effective stress of the elements of the welding surface, but one index is also proportional to fluid residence time. The results of the simulations show that both indices consistently decrease with increasing extrusion speed but behave incoherently with respect to changes in front leg shape. The parameter depending on flow velocity leads to worse results with respect to the other one, due to the excessive role played by the low velocity areas (dead zones). Both the parameters are influenced by the dead metal zones because they result from spatial averages of the variables across the welding surface.

A Lagrangian analysis of the welding paths illustrated that the welding streams do not cross the dead areas, which should consequently be excluded when computing the quality indices. This suggested a Lagrangian approach to calculate the quality indices, based on the integration of the variables along the actual welding trajectories. In this manner only the elements of the contact surface involved in the flow reconnection are taken into account. The welding quality criteria computed in the Lagrangian way, are in fully agreement with the experimental evidences: they decrease as the process speed is increased and they predict a better quality of the welding when the leg angle is smaller.

A first attempt has been carried out to explore the suitability of the Lagrangian indices also for characterizing the spatial variations of the seam weld quality along the tube thickness. The results show that the two weld seams have a different behavior: the lower seam line has a pretty constant quality along its length, while the upper line is characterized by quality change towards the peripheries. This latter behavior may be related to the microstructure of the material, which is typically characterized by coarse grains close to the external and internal surfaces and finer equiaxed grains in the interior. However, due to the contrasting results of the distribution along the two seam lines, more numerical and experimental investigation are needed to test the possible correspondence between the Lagrangian welding quality indices and the grain size distribution of the material as affected by alloy composition, temperature, strain and strain rate.

In conclusion, this study suggests that a careful analysis and selection of the welding elements is of utmost importance in the determination of the quality parameters, for the extrusion seam lines characterization. Our results support the use of a Lagrangian approach in the computation of seam weld quality indices and suggest future research on possible applications of the Lagrangian criteria to assess weld quality along the tube thickness.

ACKNOWLEDGEMENTS

We thank Carlo Conti for generating the computational grid and the C.I.L.E.A. for providing the Avogadro cluster used in the simulations.

REFERENCES

[1] G. Liu, J. Zhou, J. Duszczyk, FE analysis of metal flow and weld seam formation in a porthole die during the extrusion of a magnesium alloy into a square tube and the effect of ram speed on weld strength, J. Mater. Process. Technol. 200 (2008) 185 – 198.

[2] A. Loukus, G. Subhash, M. Imaniejad, Mechanical properties and microstructural characterization of extrusion welds in AA6082-T4, J. Mater. Sci. 39 (2004) 6561 – 6569.

[3] N. Nanninga, C. White, T. Furu, O. Anderson, R. Dickson, Effect of orientation and extrusion welds on the fatigue life of an Al-Mg-Si-Mn alloy, Int. J. Fatigue 30 (2008) 1569 – 1578.

[4] T. Sheppard, Extrusion of aluminium alloys, Kluwer Academic Publishers, Dordrecht, 1999.

[5] S. Kobayasi, S.I. Oh, T. Altan, Metal forming and the Finite Element Method, Oxford University Press, New York, 1989.

[6] J. Lof, Elasto-viscoplastic FEM simulations of the extrusion of the aluminium flow in the bearing area for extrusion of thin walled sections, J. Mater. Process. Technol. 114 (2001) 174 – 183.

[7] Duan, X. and Sheppard, T., 2003. Simulation and control of microstructure evolution during hot extrusion of hard aluminium alloys, Mater. Sci. Eng. A 351, 282 – 292.

[8] M. Schikorra, L. Donati, L. Tomesani, A.E. Tekkaya, Microstructure analysis of aluminum extrusion: Prediction of microstructure on AA6060 alloy, J. Mater. Process. Technol. 201 (2008) 156 – 162.

[9] N. Fiétier, Y. Krahenbuhl, M. Vialard, New methods for the fast simulations of the extrusion process of hot metals, J. Mater. Process. Technol. 209 (2009) 2244 – 2259.

[10] S. Støren, P.T. Moe, Extrusion, in: G. E. Totten, G.S. MacKenzie (Eds.), Handbook of aluminium Vol. I. Physical metallurgy and processes, Marcal Dekker, New York, 2003, pp. 385 – 480.

[11] G.Y. Goon, P.I. Poluchin, W.P. Poluchin, B.A. Prudcowsky, The plastic deformation of metals, Metallurgica, Moscow, 1968.

[12] O.C. Zienkiewicz, P.N. Godbole, Flow of plastic and viscoplastic solids with special reference to extrusion and forming processes, Int. J. Numer. Meth. Eng. 8 (1974) 3 – 16.

[13] S. Sibilla, A. Baron, Numerical modelling of three-dimensional aluminium flow in extrusion dies, Proceedings of 7th International Aluminum Extrusion Technology Seminar, Vol. II (2000) 203 – 210.

[14] B. Bourqui, A. Huber, C. Moulin, A. Bunetti, Improved weld seam quality using 3D FEM simulations in correlation with practice, in: Proceedings of the First EAA, European Aluminum Association-

Extruders Division, (2002), Brescia, Italy.

[15] L. Donati, L. Tomesani, The prediction of seam welds quality in aluminium extrusion, J. Mater. Process. Technol. 153 – 154 (2004) 366 – 373.

[16] L. Donati, L. Tomesani, The effect of die design on the production and seam weld quality of extruded aluminium profiles, J. Mater. Process. Technol. 164 – 165 (2005) 1025 – 1031.

[17] M. Plata, J. Piwnik, Theoretical and experimental analysis of seam weld formation in hot extrusion of aluminum alloys, Proceedings of 7th International Aluminum Extrusion Technology Seminar, Vol. I (2000), 205 – 211.

[18] C.M. Sellars, W.J.McG. Tegart, Hot workability, Int. Metall. Rev. 17 (1972) 1 – 24.

[19] Fluent User's Guide, Version 6.3, Fluent.Inc, Lebanon, 2006.

[20] R. I. Issa, Solution of implicitly discretized fluid flow equations by operator splitting, J. Comput. Phys. 62 (1986) 40 – 65.

[21] F.J. Humphreys, M. Hatherly, Recrystallization and related annealing phenomena, Elsevier Publisher, Amsterdam, 2004.

[22] R. Akeret, Properties of pressure welds in extruded aluminum alloy sections, J. Inst. Met. 100 (7) (1972) 202 – 207.

[23] H. Valberg, Extrusion welding in aluminium extrusion, Int. J. Mater. Prod. Technol., 17 (7) (2002) 497 – 556.

[24] H. Valberg, T. Loeken, M. Hval, The extrusion of hollow profiles with a gas pocket behind the bridge, Int. J. Mater. Prod. Technol. 10 (3 – 6) (1995) 222 – 267.